CD44 Controls Endothelial Proliferation and Functions as Endogenous Inhibitor of Angiogenesis

Anne Pink, Marianna Školnaja, Taavi Päll, Andres Valkna

Competence Centre for Cancer Research and Tallinn University of Technology, Akadeemia tee 15, 12618, Tallinn, Estonia

Corresponding author: Andres Valkna

Email: andres.valkna@ttu.ee

Summary

CD44 membrane glycoprotein is involved in angiogenesis, but it is not clear whether CD44 functions as a pro- or antiangiogenic molecule. Here, we assess the role of CD44 in angiogenesis and endothelial proliferation by using *Cd44*-null mice and silencing in human endothelial cells. We demonstrate that angiogenesis is increased in *Cd44*-null mice compared to either wild type or heterozygous animals. Silencing of CD44 expression in cultured endothelial cells results in augmented proliferation and viability. CD44's growth-suppressive effect is mediated by its extracellular domain and it is independent of its hyaluronan binding function. CD44-mediated effect on cell proliferation is independent of specific angiogenic growth factor stimulation. These results show that CD44 expression on endothelial cells constrains endothelial cell proliferation and angiogenesis. Thus, endothelial CD44 might serve as a therapeutic target in either cardiovascular diseases where endothelial protection is desired or, in contrast, as an antiangiogenic molecule for cancer treatment.

Introduction

Angiogenesis is a pathophysiological process involved in wound healing as well as tumor growth and metastasis. The switch of normally quiescent blood vessels to angiogenesis is determined by the balance of proangiogenic and antiangiogenic factors in tissue microenvironment. In tumor, endothelial cell (EC) proliferation and survival is regulated by growth factors such as VEGF, FGF-2, or HGF, released either by tumor cells or normal cells in the tumor stroma. Blocking proangiogenic signaling by VEGF inhibitors in tumor therapy and continuation of such therapy beyond progression shows survival benefit (Mancuso et al., 2006). However, tumors can be intrinsically resistant to anti-VEGF therapy or acquire resistance during therapy by different mechanisms (Loges et al., 2010). Better understanding of microenvironmental or EC-intrinsic factors involved in regulation of EC proliferation and blood vessel formation is needed to understand vascular biology, and to develop more effective new antiangiogenic tumor therapies.

CD44 cell-surface glycoprotein has been shown to be necessary for efficient tumor vascularization (Cao et al., 2006) and it mediates induction of angiogenesis in response to hyaluronan (HA) oligomers (Lennon et al., 2014). CD44 mediates cell adhesion to its principal ligand HA via its N-terminal HA-binding domain (HABD) (Banerji et

al., 2007; Teriete et al., 2004). CD44 and HA interaction is important in immune response where it mediates leukocyte rolling on HA during leukocyte recruitment into inflammatory site (Cuff et al., 2001; Protin et al., 1999; Rouschop et al., 2005). CD44 also mediates HA-induced effects on vasculature. Endothelial-targeted CD44 silencing *in vivo* resulted in reduced vascular density of Matrigel plug implants in response to low molecular weight-HA (Lennon et al., 2014). CD44-high molecular weight-HA interaction inhibits vascular smooth muscle cell proliferation, it has been shown that CD44-deficiency results in increased neointima formation after arterial injury (Kothapalli et al., 2007). *Cd44*-null mice display reduced vascularization of CD44-positive B16 melanoma cells containing Matrigel plugs, and reduced vessel density in B16 melanoma and ID8-VEGF ovarian carcinoma xenografts (Cao et al., 2006). However, CD44 contribution to angiogenesis *in vivo* has not been established in *Cd44*-null mice in a less complex model by using defined angiogenic growth factors instead of large numbers of tumor cells.

We have previously shown that administration of recombinant soluble CD44 hyaluronan binding domain (HABD) inhibits angiogenesis in chick chorioallantoic membrane, stimulated either by VEGF or FGF-2, tumor xenograft growth, and EC proliferation *in vitro* (Päll et al., 2004). Normal human serum contains considerable level of soluble CD44, which is even higher in mice. Increased levels of serum sCD44 have been linked to different pathological conditions, including cancer and type 2 diabetes (Kodama et al., 2012; Mayer et al., 2008; Ristamäki et al., 1994). Soluble CD44 (sCD44) is mainly a shedding product of membrane CD44 (Murakami et al., 2003; Okamoto et al., 1999). If the hypothesis of proangiogenic role of CD44 holds, then recombinant soluble CD44 HABD should function as a CD44 decoy receptor for its principal ligand HA. Nevertheless, we previously found that HA nonbinding mutant of CD44 HABD showed similar antiangiogenic and tumor growth inhibitory functions (Päll et al., 2004), suggesting that a mechanism other than HA-binding might be involved. In the current study, we sought to conclusively determine the role of CD44 in angiogenesis, and found that endothelial CD44 functions as endogenous inhibitor of angiogenesis and restrains EC proliferation.

Results

Cd44-null mice display increased angiogenic response

We studied angiogenesis in mice lacking CD44 (*Cd44*$^{-/-}$). In a preliminary experiment, we assessed Matrigel plug invasion of isolectin-B4- and CD105-positive cells in response to 50 ng/ml VEGF. Surprisingly, we found increased endothelial invasion in *Cd44*$^{-/-}$ mice compared to wild type mice (data not shown). In next series of experiments we used directed in vivo angiogenesis assay (Guedez et al., 2003) to test FGF-2/VEGF-induced angiogenic response in *Cd44*$^{-/-}$ and wild type mice from C57BL/6, C3H or mixed genetic backgrounds (Figure 1). We found a 5.4 ± 2.1 [95% CI, 2.4-10.6]-fold increase in blood vessel invasion in response to FGF-2/VEGF compared to unstimulated controls in *Cd44*$^{-/-}$ mice from mixed genetic background (one-way ANOVA $P = 0.048$, N = 2 experiments, effect size 1.2 ± 0.4 [95% CI, 0.4-2.1]; Figure 1A). Angiogenesis induction in pooled wild type mouse strains compared to unstimulated controls was 1.6 ± 0.7 [95% CI, 0.8-3.6]-fold (one-way ANOVA $P = 0.22$, N = 2 experiments, effect size 0.1 ± 0.1 [95% CI, 0-0.3]; Figure 1A, inset). When comparing growth factor stimulated groups, *Cd44*$^{-/-}$ mice displayed severalfold higher blood vessel invasion into angioreactors in response

to FGF-2/VEGF than pooled wild type mice (one-way ANOVA, $P = 0.022$), whereas unstimulated baseline values were not different. These data suggest that *Cd44* deficiency results in augmented angiogenic response. However, also factors other than CD44 might affect efficiency of angiogenesis induction in mice with different genetic backgrounds (Rohan et al., 2000).

To confirm increased angiogenesis in the absence of CD44, and to study contribution of CD44 to neoangiogenesis in genetically homogeneous inbred background, we backcrossed *Cd44*$^{-/-}$ mice six generations to C57BL/6 strain. By using littermate controls, we found significant effect of *Cd44* genotype on angiogenesis induction (ANOVA, $F_{2,42} = 3.98$, $P = 0.026$). Angiogenesis was increased in *Cd44*-null animals compared to wild types or heterozygotes. FGF-2/VEGF stimulation resulted in 2.1 ± 0.5 [95% CI, 1.3-3.3]-fold increase of blood vessel invasion in *Cd44*$^{+/+}$ C57BL/6 mice (one-way ANOVA, $P = 0.03$; effect size 0.4 ± 0.1 [95% CI, 0.1-0.7]); 1.4 ± 0.2 [95% CI, 1-2]-fold increase in *Cd44*$^{+/+}$ (one-way ANOVA, $P = 0.061$; effect size 0.2 ± 0.1 [95% CI, 0-0.4]); 2.9 ± 0.7 [95% CI, 1.8-4.8]-fold increase in *Cd44*$^{-/-}$ littermates (one-way ANOVA, $P = 0.0039$; effect size 1 ± 0.3 [95% CI, 0.4-1.5]); N = 8 mice per genotype from 2 experiments. Angiogenesis induction was associated with *Cd44* genotype in the growth factor-induced group of mice (ANOVA, $F_{2,21} = 5.45$, $P = 0.012$), whereas there was no difference in baseline vessel invasion between different *Cd44* genotypes in the unstimulated group. The post test of pairwise differences indicated that *Cd44*$^{-/-}$ mice displayed increased angiogenesis compared to either *Cd44*$^{+/-}$ or *Cd44*$^{+/+}$ littermates (Figure 1B).

We conclude from these experiments that CD44 deficiency results in augmented angiogenesis induction and therefore CD44 functions as an endogeneous angiogenesis inhibitor.

Recombinant CD44 non-HA-binding mutant Fc-fusion protein inhibits angiogenesis *in vivo*

We studied whether increasing the dose of CD44 by systemic administration of its soluble analog could suppress angiogenesis. We have previously shown that bacterially expressed GST-tagged HA-nonbinding CD44 (CD44-3MUT) inhibits angiogenesis in chick chorioallantoic membrane and subcutaneous tumor xenograft growth in mice (Päll et al., 2004). Untagged and GST-tagged CD44-3MUT display very short serum half-life limiting their potential *in vivo* use (Pink et al., 2014). Thus, in order to improve *in vivo* efficacy, we generated CD44-3MUT with a C-terminal fusion of human IgG1 Fc region (CD44-3MUT-Fc). Pharmacokinetic characterization of CD44-3MUT-Fc in rats after intravenous administration showed that its serum half-life is 17 min (Figure S1). Volume of distribution of CD44-3MUT-Fc is 18 % total body weight (%TBW), suggesting improved biodistribution compared to untagged CD44-3MUT protein (1.8 %TBW; Pink et al. (2014)).

We tested antiangiogenic effects of CD44-3MUT-Fc in athymic nude mice. Results show that FGF-2/VEGF stimulation lead to 4.5 ± 1.1 [95% CI, 3-7.2]-fold increase of blood vessel invasion into angioreactors over PBS treated control groups (t test $P = 7.7e-07$; effect size 0.8 ± 0.1 [95% CI, 0.5-1.1]; Figure 2B and C). We observed that intraperitoneal treatment of mice with CD44-3MUT-Fc inhibited FGF-2/VEGF-induced angiogenesis. In a treatment group receiving 25 mg/kg CD44-3MUT-Fc angiogenesis was inhibited to unstimulated basal level compared to growth factor induced PBS treatment group (t test $P = 1.6e-05$; effect size -0.8 ± 0.2 [95% CI, -1.1–0.5]). Administration of 0.5 or 5 mg/kg CD44-3MUT-Fc also resulted in apparent angiogenesis inhibition, but the response was less robust (Figure 2C). For recombinant protein control treatments we used irrelevant rhIgG mAb or

rhIgG-Fc. Both these molecules were purified identically to CD44-3MUT-Fc. The 0.5 mg/kg CD44-3MUT-Fc treatment showed significant inhibitory effect compared to pooled 0.5 mg/kg rhIgG/rhIgG-Fc control treatment group (t test $P = 0.034$; effect size 0.5 ± 0.2 [95% CI, 0-0.9]). Mice receiving intraperitoneally 5 or 15 mg/kg doses of rhIgG-Fc showed similar angiogenesis response as PBS and 0.5 mg/kg rhIgG-Fc control treatments, suggesting that IgG-Fc portion of CD44-3MUT-Fc is not responsible for the effects observed.

Together, our results show that systemic administration of CD44-3MUT-Fc effectively inhibits *in vivo* angiogenesis.

Soluble CD44 levels are not affected by angiogenesis

Increased levels of sCD44 are released into serum by shedding in case of inflammation or tumor growth. Previous research suggests that serum sCD44 concentration shows substantial variability between different mouse strains, and is significantly reduced (< 1 µg/ml) in severely immunodeficient mice (Katoh et al., 1994). To assess sCD44's significance in angiogenic response, we determined sCD44 concentration in serum of different wild type mouse strains, in $Cd44^{+/-}$ mice, and in athymic nude mice. Sera from $Cd44^{-/-}$ mice were used as negative controls. We found that sCD44 concentration in serum was similar in athymic nude mice and in wild type mouse strains (Figure 3A and Table 1). Soluble CD44 level in $Cd44^{+/-}$ animals was reduced in average by 35% (95% credible interval: 16-53%) compared to $Cd44^{+/+}$ mice.

To analyse whether sCD44 concentration correlates with angiogenesis induction, we excluded $Cd44^{-/-}$ mice and nude mice from dataset. We found no correlation between relative blood vessel invasion and post-experiment serum levels of sCD44 (Figure 3B). Next we evaluated whether induction of angiogenesis, rhIgG-Fc or systemic treatments with CD44-3MUT-Fc that we used in *in vivo* angiogenesis model lead to changes of sCD44 serum level in nude mice. This analysis showed that neither angiogenesis induction nor treatments had any effect on serum concentration of sCD44 in nude mice (ANOVA, $F_{11,32} = 0.975$, $P = 0.49$; Figure 3C). It also revealed that there was no correlation between post-experiment sCD44 serum concentration and vessel invasion into angioreactors independently of experimental interventions (Figure 3D).

CD44-3MUT-Fc inhibits endothelial cell proliferation and viability

To find out whether CD44-3MUT-Fc-mediated inhibition of angiogenesis is caused by its effects on ECs, we tested CD44-3MUT-Fc in a cell proliferation assay. We used cells synchronized by serum starvation to model the initial stages of stimulation of quiescent endothelial cells (Figure 4A). We applied different concentrations of CD44-3MUT-Fc to growth arrested HUVECs and released cells from arrest by stimulation with 25 ng/ml VEGF. Real-time growth curves of untreated controls show that 25 ng/ml VEGF induces robust proliferation in HUVECs that is sustained for at least 72 h (Figure 4B, leftmost facet). In contrast, CD44-3MUT-Fc treatment dose-dependently suppressed 25 ng/ml VEGF-stimulated HUVEC growth, compared to rhIgG-Fc control treatments (Figure 4B). The difference in growth kinetics between CD44-3MUT-Fc and rhIgG-Fc treatments became apparent approximately 24 h after VEGF-induced release. After this timepoint, rhIgG-Fc control-treated cells continued to proliferate, but in CD44-3MUT-Fc-treated wells cell density plateaued. Next, we used the same growth arrested HUVEC model in a cell proliferation and viability assay to compare CD44-3MUT-Fc efficacy in inhibiting cell proliferation

stimulated either by FGF-2, VEGF, or HGF (Figure 4C, D, and E). We used an endothelial-specific inhibitor of cell proliferation fumagillin as a positive control to define the maximum response in our assay. FGF-2 and VEGF induced robust proliferation in growth-arrested HUVEC, whereas HGF-stimulation resulted in much weaker induction (Figure 4C to E, left panels). Compared to rhIgG-Fc, CD44-3MUT-Fc inhibited dose-dependently HGF-stimulated proliferation with maximum response at 60% ± 12.6 of inhibition after 72 h incubation. FGF-2 or VEGF-stimulated EC growth was inhibited less efficiently by CD44-3MUT-Fc when compared to rhIgG-Fc, as growth was reduced by a maximum 10.7% ± 2.4 and 13.9% ± 4.5, respectively (Figure 4B to E, and G). These results are in agreement with respective growth factors' potency to stimulate HUVEC proliferation, CD44-3MUT-Fc inhibited less effectively FGF-2 or VEGF-induced proliferation, and showed more efficacy in case of weak inducer HGF.

CD44v6 interacts with VEGFR2 and MET (Tremmel et al., 2009). Therefore we tested whether CD44-3MUT-Fc has effect on protein levels or activation of these receptors. Western blot analysis showed no change in neither VEGFR2 nor MET protein levels or activation in response to CD44-3MUT-Fc (Figure S3). This suggests that CD44-3MUT-Fc does not cause EC growth inhibition by direct targeting of growth factor receptor signalling. Additionally, we tested CD44-3MUT-Fc effect on GDF-2 stimulated HUVEC (Figure 4D). Vascular quiescence factor GDF-2 (BMP-9) belongs to TGF-β superfamily ligands and regulates angiogenesis via ALK1, a type 1 TGF-β receptor (David et al., 2008; Scharpfenecker et al., 2007). As shown in left panel of Figure 4F, in our model GDF-2 is strongly anti-mitotic and reinforces cell-cycle block. Compared to rhIgG-Fc control treatments, CD44-3MUT-Fc showed a dose-dependent inhibitory effect on cell number in GDF-2 treated HUVEC with 79.6% ± 6.7 maximum response (Figure 4F, G).

To ascertain whether apoptosis contributes to CD44-3MUT-Fc-induced growth inhibition, we used Annexin V-FITC staining. We found that upon HUVEC release from serum starvation, basal levels of apoptosis in cell population were inversely related to the growth factors' potency to stimulate cell proliferation. In response to incubation with 12.64 μM (-4.9 $\log_{10}$ M) CD44-3MUT-Fc the number of apoptotic cells relative to pooled control treatments was increased by 9% ± 5 in VEGF, 28% ± 14 in 10%FBS, 34% ± 6 in FGF-2, 45% ± 12 in HGF, 46% ± 6 in GDF-2 stimulated cells. However, VEGF or FGF-2-induced cells were most protected against apoptosis induced by CD44-3MUT-Fc-treatment (Figure 4H). In contrast, GDF-2-mediated growth arrest enforced cells to undergo apoptosis and such trend was further increased by CD44-3MUT-Fc treatment. The observed increase in apoptosis from a relatively low basal level in response to CD44-3MUT-Fc treatment, and apparent correlation with growth factors' potency to stimulate proliferation, suggest that apoptosis occurs secondary to CD44-3MUT-Fc-mediated inhibition of cell proliferation.

Collectively, our data show that CD44-3MUT-Fc inhibits EC proliferation.

CD44 is not involved in GDF-2/ALK1-dependent SMAD signaling

Several studies suggest that CD44 associates with TGF-β signaling, since CD44 cytoplasmic tail directly interacts with SMAD1 (Peterson et al., 2004), CD44 forms a galectin-9-mediated complex with BMPR2 (Tanikawa et al., 2010), and HA induces CD44 to complex with TGFBR1 (Bourguignon et al., 2002). Given that CD44-3MUT-Fc treatment resulted in enhanced growth inhibitory effect in GDF-2 arrested HUVEC, we wanted to test whether CD44 could be involved in GDF-2 mediated SMAD activation. We studied p-SMAD1/5 nuclear localization and

SMAD1/5 target gene activation in response to GDF-2 stimulation in CD44-silenced HUVEC. As expected, we detected a robust GDF-2-dependent p-SMAD1/5 nuclear localization (Figure S2A) and induction or repression of selected known SMAD1/5 target genes ID1, SMAD6, SMAD7 or c-MYC, respectively (Figure S2B). CD44-targeting siRNA transfection resulted in substantial CD44 protein or mRNA downregulation compared to non-targeting siRNA control (Figure S2A and B, respectively). Immunofluoresence analysis showed that nuclear area or other size-shape parameters of cell nuclei did not differ between siCD44 or siNTP control-silenced cells (data not shown). We found that silencing of CD44 did not affect nuclear localization of p-SMAD1/5 or SMAD1/5 target gene expression in response to GDF-2 stimulation (Figure S2A and B).

Next, we studied CD44-3MUT-Fc effect on SMAD1/5 signaling by using a BMP-responsive element reporter (BRE). We found that BRE reporter activity in HUVEC was increased in response to GDF-2 stimulation, but this response was not sensitive to either CD44-silencing or CD44-3MUT-Fc treatment (Figure S2C). In line with this, western blot analysis of GDF-2 stimulated HUVEC treated with CD44-3MUT-Fc showed no change in p-SMAD1/5 levels (Figure S2D). To test whether prolonged CD44-3MUT-Fc exposure *in vivo* could trigger changes in SMAD1/5-mediated gene expression, we analysed lung tissue of nude mice from two angiogenesis experiments described in Figure 2 for expression of selected SMAD target genes. We found no changes in expression levels of SMAD1/5 and NF-κB target genes (Figure S2E).

Together, these results suggest that CD44 or CD44-3MUT-Fc are not involved in GDF-2-ALK1-SMAD1/5 signaling in ECs.

CD44 silencing augments endothelial cell proliferation

Based on angiogenesis assay results showing increased blood vessel invasion in *Cd44*$^{-/-}$ mice and inhibition of this response by CD44-3MUT-Fc treatment, we wanted to test whether CD44 knockdown in ECs results in increased cell growth. To this end, we used siRNA transfected HUVECs that had been growth arrested by serum starvation. Growth-arrested cells were released by addition of either 20% FBS or different concentrations of VEGF or FGF-2. Real-time impedance measurements showed that compared to 5% FBS stimulation (Figure 5A, left), 20% FBS or growth factor supplementation released cells from cell-cycle block and stimulated their growth sustainably over 72 h (Figure 5A, C). We found that siCD44 transfected cells reached higher densities at 72 h than control siNTP-transfected cells. Augmented cell growth and higher cell density in siCD44-transfected ECs at the end of experiment was independent of type and concentration of the growth factor used for stimulation (Figure 5A, C, and E). End-point quantitation of viable cells performed 72 h after release supported impedance measurement result. siCD44-transfected HUVECs displayed increased cell numbers over all tested growth factors and concentrations (Figure 5B, D). These data suggest that the effect of CD44 silencing on cell proliferation was additive to the stimulatory effect of growth factors. The additive effect of CD44 silencing on cell proliferation was further supported by the observation that, in case of VEGF-stimulated HUVEC, the typical VEGF dose-dependent suppression of growth maximum persisted. In case of FGF-2, such suppression did not occur and cell density increased linearly with growth factor concentration within the range (8 to 79 ng/ml) tested.

Western blot analysis showed that growth factor receptor levels were not affected in CD44-silenced HUVEC (Figure 5G). The initial proliferation rate of CD44-silenced HUVECs after seeding and before serum deprivation was increased compared to non-targeting siRNA or untransfected controls and CD44-silenced cells reached higher

cell density within this timeframe (Figure S4A). Notably, vimentin-silenced HUVEC showed similar behavior to CD44-silenced cells before serum starvation (Figure S4A). The observation that siCD44- or siVIM-transfected HUVEC reached higher cell density after seeding, and before start of serum starvation, compared to siNTP-transfected or untransfected cells was confirmed by modeling impedance data for barrier formation (Figure S4B). The release of siCD44-transfected cells from serum starvation by VEGF or FGF-2 stimulation resulted in enhanced barrier re-formation when compared to siNTP or siVIM-transfectants (Figure S4B).

We also assessed the effect of siCD44 when cell cycle G1-phase arrested cells were treated with anti-mitogenic factor GDF-2. We found that GDF-2 enforces cell cycle-block and a subsequent decline in cell density, plausibly because cells undergo apoptosis (Figure 3H). Impedance measurements showed that CD44-silencing did not rescue GDF-2-stimulated HUVEC from growth arrest and cell numbers declined over the course of experiment (Figure 5E). However, cell viability assay performed at the end of impedance measurements showed that CD44-silencing resulted in more surviving cells compared to controls and partially rescued the GDF-2 effect (Figure 5F). Nevertheless, GDF-2 dose-dependent inhibitory trend persisted.

Together, these experiments show that CD44 knockdown results in enhanced EC proliferation, independent of specific growth factor used for stimulation. Furthermore, CD44-silencing experiments are consistent with *Cd44*$^{-/-}$ mice data and suggest increased proliferation and survival of CD44-deficient ECs as plausible cellular mechanism resulting in enhanced angiogenesis.

Discussion

Here we report that CD44 cell-surface glycoprotein is a negative regulator of angiogenesis. We show that CD44 constrains endothelial cell proliferation. Our results suggest that CD44 functions in regulation of cell proliferation independently of specific growth factor signaling pathway.

Here we extend the functions of CD44 to the control of EC proliferation and angiogenesis. We found that blood vessel invasion into tumor ECM in response to FGF-2/VEGF stimulation was substantially increased in *Cd44*-null mice. This effect is likely cell-autonomous, as silencing of CD44 expression in cultured ECs also resulted in augmented cell proliferation. We suggest that CD44 functions downstream of mitogenic signaling. Griffioen et al. (1997) have showed that CD44 is upregulated in response to FGF-2 or VEGF stimulation in cultured ECs, and in activated tumor blood vessels *in vivo*. Thus, enhanced angiogenesis and cell proliferation in case of CD44 deficiency or downregulation suggest that CD44 mediates negative feedback signaling that constrains cell proliferation. CD44 knockdown in dermal fibroblasts results in stabilization of PDGF β-receptor and sustained ERK activation in response to PDGF-BB stimulation (Porsch et al., 2014). Here we show that intervening with CD44 function by silencing or CD44-3MUT-Fc has no effect on activation of angiogenic growth factor receptors. However, we observed that CD44-3MUT-Fc's potency to inhibit EC proliferation was inversely related to the potency of VEGF, FGF-2, or HGF to induce EC proliferation and survival. Several earlier reports show involvement of CD44 in TGF-β signaling (Bourguignon et al., 2002; Peterson et al., 2004; Tanikawa et al., 2010). Thus, we tested if CD44 functions in GDF-2 signaling. We saw enhanced growth arrest and apoptosis of ECs in response to CD44-3MUT-Fc treatment in GDF-2-stimulated ECs. Nevertheless, our different *in vitro* experiments showed that GDF-2-mediated signaling is not affected by disrupting CD44 expression or increasing CD44 dose via CD44-3MUT-Fc. We conclude from these results that CD44 acts via a different mechanism than disrupting any

specific growth factor pathway.

Plausibly, CD44-mediated negative feedback signaling on cell proliferation is activated by CD44-HA interaction. Binding of high molecular weight HA to CD44 controls proliferation of smooth muscle cells, and probably also other mesenchymal cell types, including ECs (Kothapalli et al., 2007). Kothapalli et al. (2007) also showed that in *Cd44*-null mice the response to arterial injury resulted in increased neointima formation and smooth muscle cell proliferation during vessel regeneration. We have previously shown that HA non-binding mutant of CD44 was as effective as its wild type counterpart in angiogenesis inhibition in chick chorioallantoic membrane angiogenesis model (Päll et al., 2004). Here, we show that systemic administration of soluble mutant CD44 HABD (CD44-3MUT) has an antiangiogenic effect in a mouse model of angiogenesis, thus CD44-3MUT functions similarly to endogeneous CD44. In this context, we were interested whether endogeneous soluble CD44 levels correlate with angiogenesis. Soluble CD44 levels are reduced in immune deficient BALB/c.Xid with defective B-cell maturation, and in SCID mice with absence of functional T cells and B cells, suggesting that immune cell derived proteolytic activity is responsible for CD44 shedding (Katoh et al., 1994). In our angiogenesis assays, we observed that wild type mouse strains displayed much weaker angiogenic response than immune deficient athymic nude mice. Given that nude mice carry normal *Cd44* gene dose, but their sCD44 levels were not known, we assumed that elevated angiogenesis in nude mice, compared to wild type strains, could be related to decreased sCD44 levels. We found serum sCD44 levels to be normal in athymic nude mice, suggesting that induction of angiogenesis is not related to serum sCD44 levels. Furthermore, as athymic nude mice lack T-cells, this result suggests that a large proportion of serum sCD44 is generated by B-cell dependent activity.

The signaling pathway downstream of CD44 is not well understood. CD44 has been implicated in cell–cell contact inhibition in schwannoma cells by recruiting NF2 tumor suppressor protein to plasma membrane (Morrison et al., 2001). Thus, it is possible that CD44 silencing abolishes NF2 function, which leads to loss of contact inhibition and increased proliferation. However, embryonic fibroblasts isolated from *Cd44*-null mice still exhibit functional contact inhibition compared to cells from *Nf2*-null mice, but *Cd44*-null cells seem to display faster growth rate compared to wild type cells (Lallemand et al., 2003). Our impedance-based real-time monitoring of cell proliferation suggest steadily increased growth rate of CD44-silenced EC after release from serum starvation. We found that barrier formation, which is directly related to cell density, is apparently more robust in CD44-silenced ECs after growth factor stimulation. This suggest that mechanisms other than defective cell–cell adhesion could be behind enhanced cell proliferation.

Our *in vivo* findings contrast with previous works showing that CD44 absence or its downregulation *in vivo* results in reduced angiogenesis (Cao et al., 2006; Lennon et al., 2014). Lennon et al. (2014) studied CD44 contribution to HA oligomer induced angiogenesis, and CD44 silencing *in vivo* resulted in inhibited angiogenesis in response to oligo HA. Cao et al. (2006) used a relatively high number of rapidly growing B16 melanoma cells as a source of angiogenic growth factors in a Matrigel plug assay and allowed the blood vessels to grow for 5 days only. Nevertheless, tumor angiogenesis assays using two different cell lines with very different tumor growth kinetics, B16 melanoma and ID8-VEGF ovarian carcinoma, still suggested considerable inhibition of tumor formation and reduced vascular density at tumor margins in *Cd44*-null mice (Cao et al., 2006). However, it is plausible that CD44-negative ECs were inhibited *in trans* by CD44 that was present on tumor cells (Cao et al., 2006). Here we

show that administration of exogeneous soluble CD44 inhibited *in vivo* angiogenesis and EC proliferation. We found that *Cd44* heterozygous mice displayed angiogenesis at similar level as wild type animals, showing that *Cd44* is not haploinsufficient and lower than normal amounts are still sufficient for controlling angiogenesis. Tumor angiogenesis is dependent on interactions between tumor cells and host tissue stroma, and such interactions might be compromised in *Cd44*-null animals. Tumor cells recruit macrophages to promote angiogenesis. However, Cao et al. (2006) showed that in case of *Cd44*-null mice bone marrow reconstitution with wild type bone marrow did not repair angiogenesis defect, suggesting that endothelial CD44 expression is important.

Cd44-null mice develop normally and do not display apparent vascular abnormalities. We suggest that CD44 plays a non-redundant role in physiological angiogenesis. CD44-mediated interactions after its upregulation in endothelial cells in response to growth factor stimulation restrain cell proliferation. Such control may contribute to robust shutdown of angiogenesis during wound repair. In case of tumors, CD44-mediated control of angigenesis might be overridden by surplus of growth factors and increased shedding of CD44.

In summary, we conclude that CD44 functions as a negative regulator of angiogenesis. Therefore systemic absence of CD44 expression in mice results in increased angiogenic response. Our results also demonstrate that soluble CD44 regulates angiogenesis by suppressing endothelial cell proliferation. Importantly, CD44 antiangiogenic effect is achieved independently of its HA binding property. Together, our data suggest that CD44 is important in maintaining normal angiogenesis levels and targeting of CD44 can be utilized in antiangiogenesis treatment strategies in cancer or in other applications where angiogenesis modulation is desired.

Experimental Procedures

Cells, Reagents and Primary Antibodies

HUVEC were from Cell Applications, Inc. , ECGS was from Millipore. VEGF-165 was from Serotec, GDF-2, HGF and FGF-2 were from Peprotech. Lipofectamine RNAiMAX (LF) was from Life Technologies. Non-targeting pool siRNA, #D-001810-10-05, human CD44 siRNA, #L-009999-00-0005, and human vimentin siRNA, #L-003551-00-0005 (ON-TARGETplus SMARTpool) were from Thermo Fisher Scientific. siRNA target sequences are listed in Supplemental Experimental Procedures. jetPEI-HUVEC transfection reagent was from PolyPlus-transfection. Annexin V-FITC and annexin binding buffer were from BD Pharmigen. CellTiter-Glo reagent was from Promega. Primary antibodies, dilution and source used in this study: anti-CD44 (2C5) mouse mAb 1/1000 from R&D Systems, anti-VEGFR2 rabbit mAb (55B11) 1/1500 and anti-FGFR1 rabbit mAb (D8E4) from Cell Signaling Technology and anti-vimentin (V9) mouse mAb 1/3000 (Santa Cruz Biotechnology). IM7 rat anti-mouse CD44 (MCA4703, AbD Serotec), rat anti-mouse CD44 KM81-biotin (Abcam).

Production of CD44-3MUT-Fc

CD44-3MUT with C-terminal human IgG1-Fc domain, recombinant human IgG1-Fc domain (rhIgG-Fc) and irrelevant human IgG1 mAb were produced by Icosagen Cell Factory (Estonia). Cystatin S signal peptide sequence was added to N-terminus of the CD44-3MUT-Fc cDNA and the gene was synthesized by Genewiz, Inc. The

synthesized CD44-3MUT-Fc cDNA was cloned into RSV-LTR promoter containing pQMCF-5 expression vector (Icosagen Cell Factory). Resulting expression plasmids were transfected into CHOEBNALT85 cells (Icosagen Cell Factory) and expressed Fc-fusion proteins were purified by Protein G sepharose, followed by Superdex 200 gel-filtration chromatography. Purified CD44-3MUT-Fc has a monomeric molecular weight approximately 60 kDa. The endotoxin level of purified CD44-3MUT-Fc was < 10 EU/mg as determined by chromogenic Limulus amebocyte lysate test (Lonza).

In Vivo Angiogenesis Assay

Animal experiments were conducted under the license of Estonian Ministry of Agriculture ethical review committee. We used Directed in Vivo Angiogenesis Assay kit (DIVAA; Trevigen, USA) according to manufacturers instructions. For angiogenesis assay, 20 µl angioreactors were filled with growth factor reduced basement membrane extract containing 1.4 ng/µl FGF-2, 0.47 ng/µl VEGF and heparin for the induction of angiogenic response, or equal volume of PBS for uninduced controls. Angioreactors were implanted subcutaneously into dorsolateral flank of 9 week old athymic Nude-Foxn1/nu female mice (Harlan, Netherlands). *Cd44*-null mice were from mixed inbred background (B6;129-Cd44tm1Hbg/J), termed "Cd44KO mix". B6;129 hybrid mice "WT mix" were used as controls. C57BL/6 and C3H mice were from Harlan, Netherlands. The experimental groups of wild type and *Cd44*-null mice comprised 8-11 weeks old female and male mice. In one experiment, Cd44KO mix and respective wild type mice were 40-43 weeks old. For angiogenesis assay in C57BL/6 genetic background, *Cd44*-null allele was backcrossed for six generations to C57BL/6 mice (Harlan, Netherlands); experimental groups contained equal number of female and male littermates. Implantation was performed on both flanks and one or two angioreactors were inserted per flank for immune competent mice or nude mice, respectively. Nude mice were injected intraperitoneally every second day with CD44-3MUT-Fc, irrelevant human IgG1 mAb, rhIgG-Fc or vehicle (PBS) during two weeks. Mice were sacrificed after 14 days from start of the experiment by carbon dioxide asphyxiation and angioreactors were dissected. Angioreactor contents were retrieved and angioreactor-invaded ECs were quantitated by FITC-Lectin staining. Cell-bound fluorescence was measured at 485 nm excitation and 535 nm emission wavelengths using a microtiter plate reader (Tecan, Swizerland). Data from irrelevant human IgG1 mAb and rhIgG1-Fc treatments were pooled for analysis. Raw fluorescence values from each experiment were scaled by dividing with their root mean square.

Mouse sCD44 ELISA

For quantification of sCD44 serum level nude mice from DIVAA experiments, wild type mice from different backgrounds (C3H,C57BL/6, mixed), and *Cd44*-null, heterozygous and wild type littermates in C57BL/6 background were used. For ELISA measurement 96-well plates were coated with 50 ng IM7 Ab/well at 4°C overnight (ON) and blocked with 5% non-fat dry milk for 2 h at 37°C. After blocking, samples and standards (Recombinant Mouse CD44 Fc Chimera; R&D Systems) were incubated in wells for 30 min at 37°C. Bound sCD44 was detected by incubating plate with KM81-biotin Ab for 30 min at 37°C. For color development, Vectastain ABC (Vector Laboratories) and tetramethylbenzidine substrate was used. Absorbance was recorded at 450 nm using a microtiter plate reader (Tecan).

HUVEC Growth and Treatments

HUVEC (passage 4-6) were cultured in 20% FBS containing M199 medium supplemented with 4 mM L-glutamine, 50 µg/ml heparin, 10 mM Hepes, 30 µg/ml ECGS. For treatments, HUVEC were seeded into 0.1% gelatin-coated cell culture plates. After 24 h cells were starved in M199 media supplemented with 1% FBS, 25 mM Hepes and 4 mM L-glutamine for ON. After starving cells were incubated with different concentrations of rhIgG-Fc or CD44-3MUT-Fc in 5% FBS containing HUVEC growth media (5% FBS, M199, 4 mM L-glutamine, 12.5 µg/ml heparin, 10 mM Hepes, 7.5 µg/ml ECGS) for 1 h at 37°C and thereafter stimulated with 25 ng/ml of VEGF-165, 25 ng/ml of FGF-2, 10 ng/ml GDF-2 or 63 ng/ml HGF. The cells were further grown for 48 or 72 h at 37°C.

Electric Cell-Substrate Impedance Assay

Cell layer impedance was recorded by an ECIS Zθ instrument connected to a computer running an ECIS software version 1.2.169.0 (Applied Biophysics, USA). We used 96WE1+ PET plates, pretreated with 10 mM cysteine (Applied Biophysics, USA). HUVEC were seeded at a density of 5000 cells/well. The final media volume during treatments was 175 µl per well. Cell growth was monitored at seven frequencies in the range of 1000-64000 Hz. Each well was measured approximately four times per hour. To summarise different experiments, values for each experiment were binned by hours and hourly means were calculated. Release mark from serum starvation was set as time point zero. Hourly means of raw readings were normalised by dividing with the mean value of first hour after time point zero.

Apoptosis and Cell Viability Assays

For apoptosis assay HUVEC were cultured in 0.1% gelatin-coated 24-well plates at density 25000 cells/well. Annexin V-FITC staining was performed according to manufacturer's protocol. Briefly, cells were incubated with 1:20 Annexin V-FITC in 50 µl of annexin binding buffer for 15 min at room temperature (RT) in dark and analysed by FACS Calibur (BD Biosciences). For cell viability assay, HUVEC were cultured in 0.1% gelatin-coated white 96-well cell culture plates (Greiner Bio-one) at a density of 5000 cells/well. After treatments cells were incubated with CellTiter-Glo reagent (1:1 vol to media) for 10 min at RT and luminescence was recorded using a microtiter plate reader. For analysis, raw luminescence values were min-max normalised. Curves were fitted using five parameter logistic equation: $f(x) = Bottom + \frac{Top-Bottom}{(1+\exp(HillSlope(\log(x)-\log(EC50))))^S}$.

HUVEC Transfection with siRNAs

siRNA transfections were performed using PEI or LF and 30 nM siRNAs. Transfection reagents and siRNAs were separately diluted in serum free DMEM (high glucose). Diluted siRNA and transfection reagents were mixed and transfection complex was incubated for 15-20 min at RT. The cells were transfected in 2% FBS and 4 mM L-glutamine containing DMEM (high glucose) for 3 h (PEI transfection) or 4 h (LF transfection) at 37°C. The transfection media was replaced with 20% FBS HUVEC culture media and cells were further incubated for 24 h at 37°C. For impedance measurements, the transfected cells were plated out at a 5000 cells/well density into cysteine pretreated and gelatin coated 96WE1+ PET plates. After starving, cells were stimulated with different

concentrations of GDF-2, VEGF, or FGF-2 in 5% FBS containing HUVEC growth media. After 72 h of incubation CellTiterGlo reagent was added to cells for cell viability measurement.

Western Blot Analysis

24 h after siRNA transfection cells were lysed in RIPA buffer (50 mM Tris pH 8.0, 150 mM NaCl, 1% NP-40, 0.5% sodium deoxycholate, 0.1% SDS) containing protease inhibitor coctail (Roche). The proteins (10 µg of total protein) were separated on 7.5-10% SDS-PAGE gradient gel and transferred to PDVF membrane at 350 mA 1.5 h. The membranes were blocked in 5% whey in 0.1% Tween20-TBS (TBST) at RT for 1 h, followed by a primary Ab incubation ON at 4°C and subsequent HRP- conjugated secondary Ab (Jackson Immunoresearch) incubation for 1 h at RT in 2% whey-TBST.

Statistical Analysis

We used R version 3.2.3 (2015-12-10) for data analysis and graphs (for complete list of packages see Supplemental Experimental Procedures). The percentile confidence intervals were obtained using nonparametric bootstrap resampling on 1000 replications. Cohen's d effect-sizes with bootstrap confidence intervals were calculated using bootES 1.2 package. Bayesian credible intervals were obtained via Markov chain Monte Carlo method using rjags 4.5 package. Data are shown as mean ± SEM.

Author Contributions

Conceptualization, A.P., T.P., and A.V.; Methodology, A.P., M.S., and T.P.; Investigation, A.P., M.S., and T.P.; Formal Analysis, and Visualitation, T.P.; Writing – Original Draft, A.P. and T.P.; Writing – Review & Editing, A.P., M.S., T.P., and A.V.; Funding Acquisition, A.V; Supervision, T.P., and A.V.

Acknowledgments

We are grateful to Kati Mädo for her contribution to half-life studies and Aili Kallastu for her contribution to half-life and animal studies. We thank Richard Tamme for proofreading of the manuscript. This research was supported by the European Regional Development Fund via Enterprise Estonia grants (EU28138/EU28658, EU30013) to Competence Centre for Cancer Research and by Estonian Science Fund Grant PUT698 to Andres Valkna. The authors declare no competing financial interests.

Figures and Tables

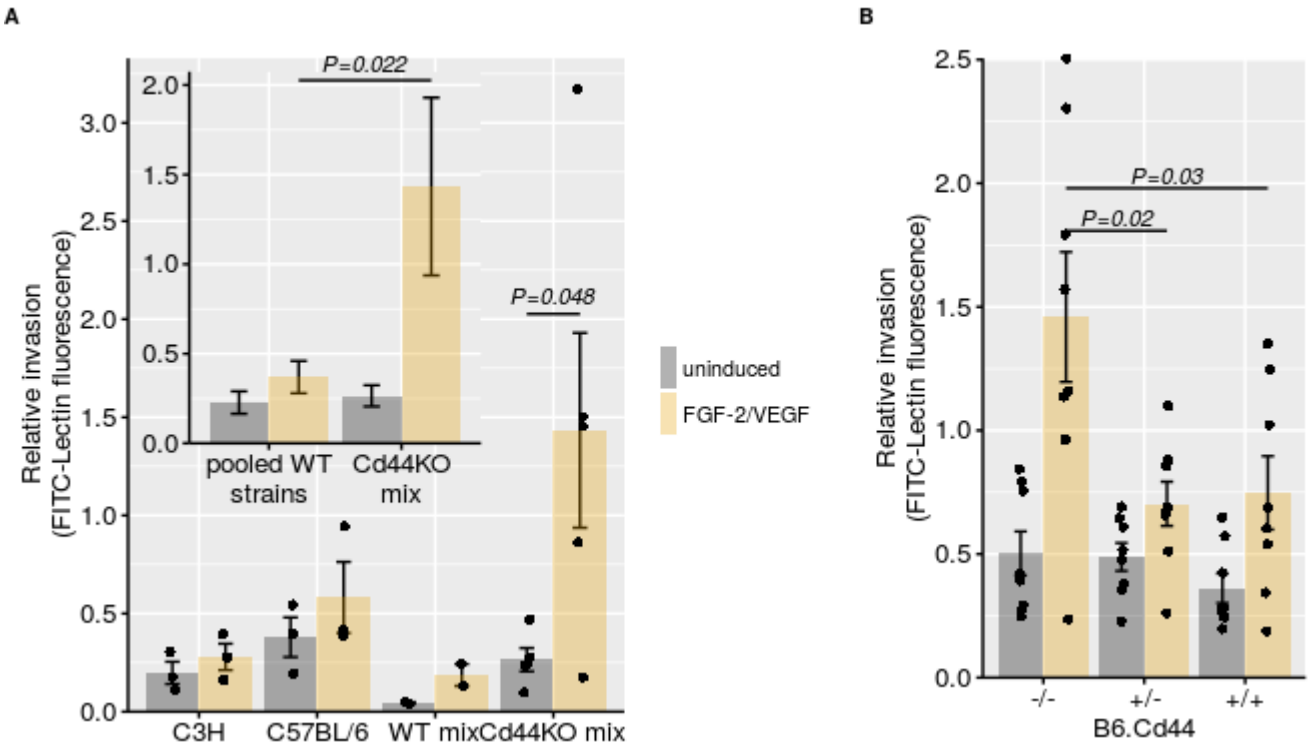

Figure 1. **Increased angiogenesis in CD44-deficient mice**. (**A**) Angiogenesis was analysed in C3H, C57BL/6, and *Cd44*-null mice in mixed genetic background (Cd44KO mix). Basement membrane extract filled angioreactors containing premixed FGF-2, VEGF and heparin or PBS for uninduced controls were implanted SC into flanks of mice. Each mouse received 2 angioreactors, 1 per flank. 14 days after implantation, angioreactors were resected and the population of ECs within the angioreactor matrix was assessed by FITC-lectin staining. The number of fluorescent cells was quantitated by microplate reader. Background subtracted raw readings from experiments were scaled by division with quadratic mean. N = 2–5 mice per condition from 2 independent experiments. P values are from one-way ANOVA. (**B**) Angiogenesis in $Cd44^{-/-}$ mice, heterozygous ($Cd44^{+/-}$), or wild type ($Cd44^{+/+}$) littermates bred six generation into C57BL/6 background. Data are represented as mean ± SEM. Each dot represents the mean of two angioreactors for an individual mouse. N = 8 mice per condition from 2 independent experiments. P values are from ANOVA post hoc comparisons using the Tukey HSD test.

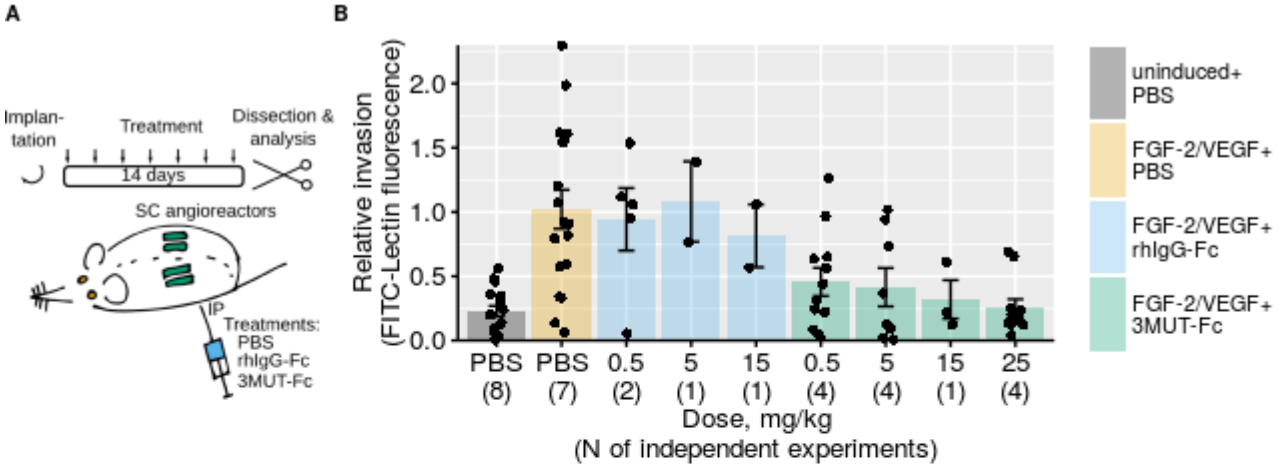

C

	uninduced + PBS	GF + vehicle	GF + rhIgG-Fc 0.5 mg/kg	GF + 3MUT-Fc 0.5 mg/kg	GF + 3MUT-Fc 5 mg/kg
GF + PBS	0.8 (0.5-1.1), 7.7e-07				
GF + rhIgG-Fc 0.5 mg/kg	0.7 (0.2-1.1), 0.0017	-0.1 (-0.6-0.4), 0.72			
GF + 3MUT-Fc 0.5 mg/kg	0.2 (0-0.5), 0.16	-0.6 (-0.9--0.2), 0.00075	0.5 (0-0.9), 0.037		
GF + 3MUT-Fc 5 mg/kg	0.2 (-0.1-0.5), 0.31	-0.6 (-1--0.2), 0.0014	-0.5 (-1-0.1), 0.034	0 (-0.4-0.3), 0.83	
GF + 3MUT-Fc 25 mg/kg	0 (-0.1-0.2), 0.86	-0.8 (-1.1--0.5), 1.6e-05	0.7 (0.2-1.1), 0.0042	0.2 (-0.1-0.5), 0.27	0.2 (-0.1-0.5), 0.43

Figure 2. **Recombinant CD44-3MUT Fc fusion protein inhibits angiogenesis *in vivo***. Assay and quantitation was performed essentially as in Figure 1, except each mouse received 4 angioreactors, 2 per flank. The day after implantation mice started to receive CD44-3MUT-Fc, control rhIgG1-Fc or vehicle (PBS) every second day via IP injections for 14 days. (**A**) Schematic presentation of experimental design. (**B**) Relative blood vessel invasion into matrix filled angioreactors. Data are represented as mean ± SEM. Datapoints show the mean of 4 angioreactors for individual mice. N, number of independent experiments. GF, growth factors (FGF-2/VEGF). (**C**) Effect size with 95% confidence intervals (upper row) and P-values (lower row) of pairwise comparisons of data shown in (**B**). Effect sizes were calculated by Cohen's d formula. Confidence intervals were derived using bootstrap resampling. P values are from t tests using pooled SD. See also Figure S1.

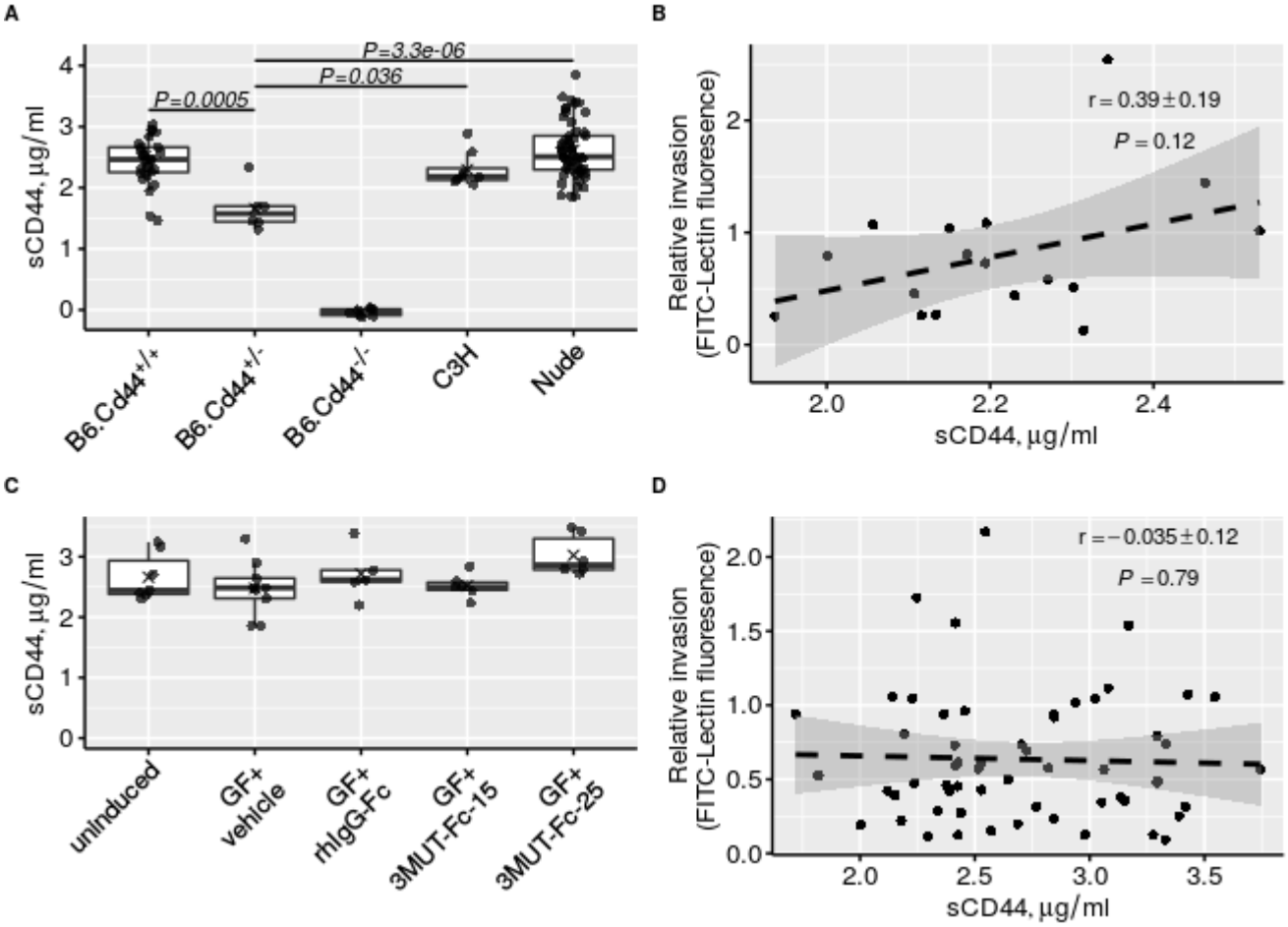

Figure 3. **Soluble CD44 concentration in mouse serum**. Blood was collected from mice of different genetic backgrounds and mice used in angiogenesis experiments shown in Figures 1 and 2. (**A**) Serum soluble CD44 levels in mice from different strains. Each dot represents an individual mouse. Cross indicates mean. P values are from ANOVA post hoc comparisons using the Tukey HSD test. (**B**) The correlation between relative blood vessel invasion and post experiment serum sCD44 in wild type mice. *Cd44*-null mice and nude mice were excluded from dataset. Pearson's r and associated P value is shown. (**C**) Levels of sCD44 in serum of nude mice from different treatment groups determined post experiment. Treatments where more than five mice were analysed are shown. Each dot represents an individual mouse. Cross indicates mean. GF, growth factors (FGF-2/VEGF). (**D**) The correlation between relative blood vessel invasion and post experiment serum sCD44 in nude mice. Pearson's r and associated P value is shown. (**B** and **D**), dashed line is linear model fit, gray shading is standard error interval of fitted values.

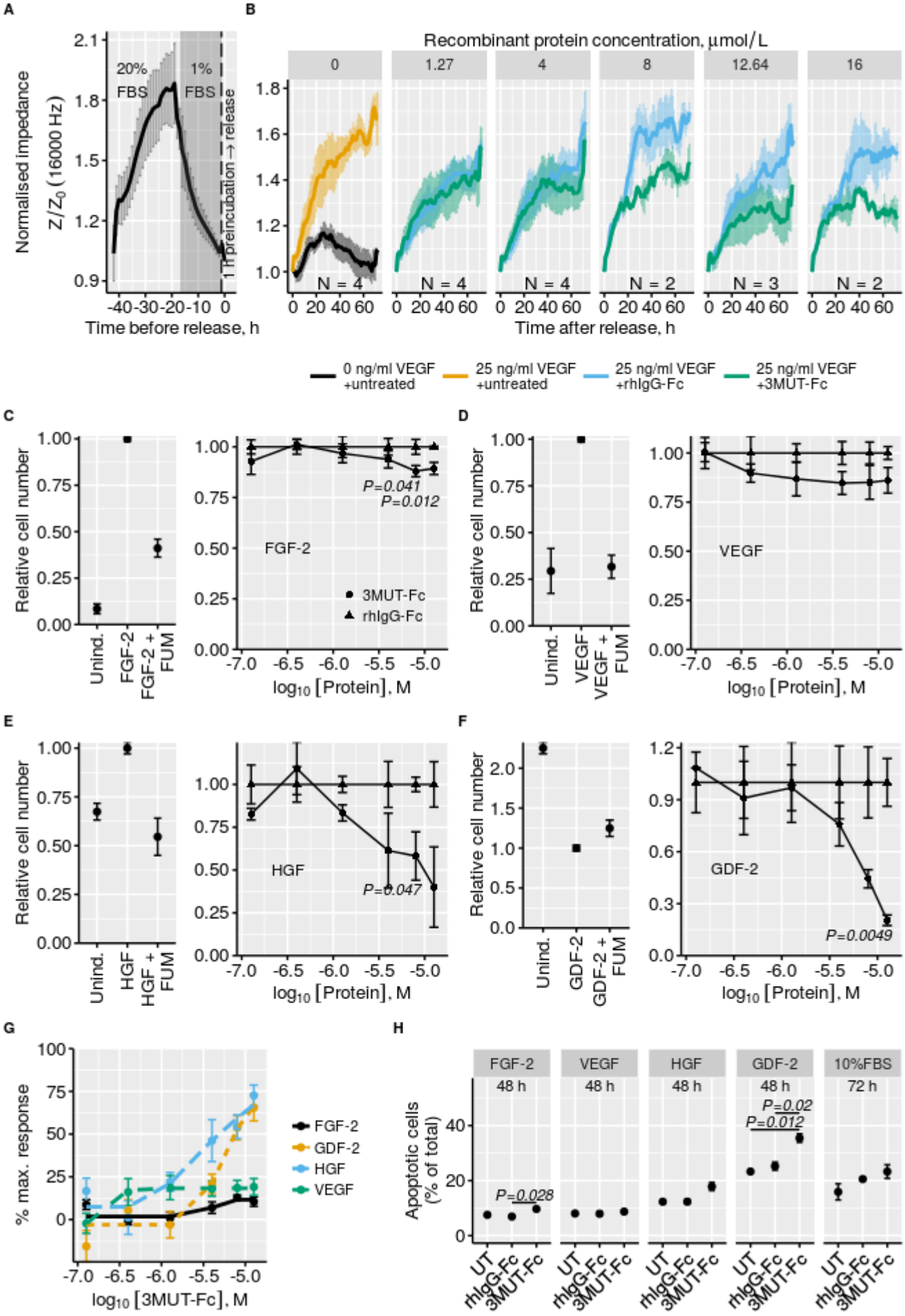

Figure 4. **CD44-3MUT-Fc inhibits EC growth**. (**A**) Real-time track of cell adhesion and synchronisation of HUVECs seeded onto 96-well electrode arrays. After seeding, cells were grown for about 24 h. After which cells were starved overnight in media supplemented with 1% FBS (gray area). 1 h before release from serum starvation (vertical dashed line) cells were preincubated with different concentrations of rhIgG-Fc or CD44-3MUT-Fc in 5% FBS containing media. (**B**) Growth curves of HUVEC released from serum starvation by supplementing preincubation media with 25 ng/ml VEGF. Facet labels show rhIgG-Fc or CD44-3MUT-Fc concentration during preincubation. Data are represented as mean ± SEM. N, number of independent experiments. (**C–F**) HUVECs were synchronised and pretreated as in panel A. After preincubation cells were stimulated either with 25 ng/ml FGF-2 (**C**), 25 ng/ml VEGF (**D**), 63 ng/ml HGF (**E**) or 10 ng/ml GDF-2 (**F**). After 72 h, the number of viable cells was quantitated by measuring ATP per well. Left, the effect of growth factor stimulation and the effect of 10 nM fumagillin (FUM) as a positive control for inhibition of cell proliferation. Right, the dose-response curves of rhIgG-Fc (filled triangles) or CD44-3MUT-Fc (filled circles). Data are represented as mean ± SEM. N = 3–4 independent experiments. (**G**) CD44-3MUT-Fc dose-response curves for FGF-2, GDF-2, HGF or VEGF stimulated HUVEC. Data are represented as mean ± SEM. (**H**) Apoptosis of HUVECs stimulated with different growth factors and treated with 12.64 µM (-4.9 $\log_{10}$ M) rhIgG-Fc, CD44-3MUT-Fc or left untreated. Apoptosis was quantitated by Annexin V staining. Data are represented as mean ± SEM. N = 2 independent experiments. P values are from ANOVA post hoc comparisons using the Tukey HSD test. See also Figure S2 and S3.

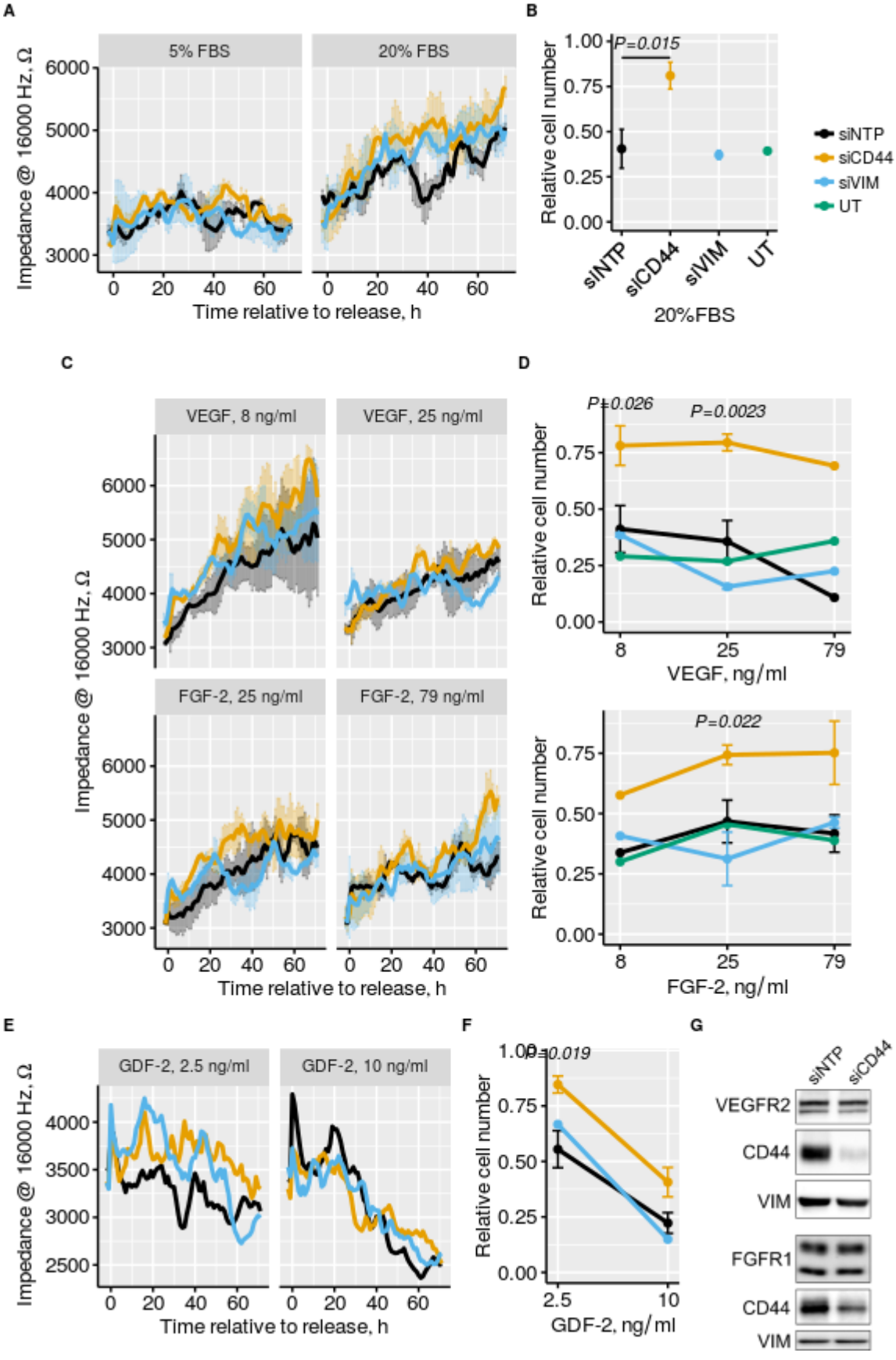

Figure 5. **CD44 knockdown augments EC growth**. siRNA transfected HUVECs were plated onto 96-well electrode arrays. After 24 h, cells were starved in 1% FBS media for overnight. After starving, cells were released from cell cycle block by addition of 20% FBS **(A)**, 8, 25, or 79 ng/ml of FGF-2 or VEGF **(C)**, and 2.5 or 10 ng/ml GDF-2 **(E)**. Following stimulation, HUVEC growth was monitored by recording electrode impedance. Raw impedance readings are shown to allow direct comparison to endpoint measurements. N = 2 for 5% and 20% FBS,

25 and 79 ng/ml FGF-2, and 8 and 25 ng/ml VEGF. **(B, D, F)** 72 h after release from cell cycle block the viable cell numbers were determined by measuring ATP per well. Treatments are labeled as shown in (**B**). Data are represented as mean ± SEM. P values are from ANOVA post hoc comparisons using the Tukey HSD test. P values ≤ 0.05 of siCD44-siNTP comparisons are shown. siCD44-siNTP comparisons, N = 4 for 2.5 and 10 ng/ml GDF-2, and N = 5 for 20% FBS, 25 and 79 ng/ml FGF-2, 8 and 25 ng/ml VEGF. **(G)** Western blot analysis of CD44 silencing in HUVECs transfected with 30 nM siRNAs for 48 h. siNTP - non-targeting siRNA pool, siVIM - vimentin-targeting pool, siCD44 - CD44-targeting pool, UT - non-transfected cells. See also Figure S4.

Table 1. Soluble CD44 level in mouse serum. Concentration is shown as mean ± SEM.

Strain	sCD44, µg/ml	N	95% credible interval
B6	2.4 ± 0.07	28	2.3-2.6
B6.Cd44$^{+/-}$	1.7 ± 0.1	6	1.2-2.1
C3H	2.3 ± 0.1	8	2-2.6
Nude	2.6 ± 0.06	55	2.5-2.7

References

Banerji, S., Wright, A.J., Noble, M., Mahoney, D.J., Campbell, I.D., Day, A.J., and Jackson, D.G. (2007). Structures of the CD44-hyaluronan complex provide insight into a fundamental carbohydrate-protein interaction. Nat Struct Mol Biol *14*, 234–239.

Bourguignon, L.Y., Singleton, P.A., Zhu, H., and Zhou, B. (2002). Hyaluronan promotes signaling interaction between CD44 and the transforming growth factor beta receptor I in metastatic breast tumor cells. J. Biol. Chem. *277*, 39703–39712.

Cao, G., Savani, R.C., Fehrenbach, M., Lyons, C., Zhang, L., Coukos, G., and Delisser, H.M. (2006). Involvement of endothelial CD44 during in vivo angiogenesis. Am J Pathol *169*, 325–336.

Cuff, C.A., Kothapalli, D., Azonobi, I., Chun, S., Zhang, Y., Belkin, R., Yeh, C., Secreto, A., Assoian, R.K., Rader, D.J., et al. (2001). The adhesion receptor CD44 promotes atherosclerosis by mediating inflammatory cell recruitment and vascular cell activation. J Clin Invest *108*, 1031–1040.

David, L., Mallet, C., Keramidas, M., Lamande, N., Gasc, J.M., Dupuis-Girod, S., Plauchu, H., Feige, J.J., and Bailly, S. (2008). Bone morphogenetic protein-9 is a circulating vascular quiescence factor. Circ. Res. *102*, 914–922.

Griffioen, A.W., Coenen, M.J., Damen, C.A., Hellwig, S.M., Weering, D.H. van, Vooys, W., Blijham, G.H., and Groenewegen, G. (1997). CD44 is involved in tumor angiogenesis; an activation antigen on human endothelial cells. Blood *90*, 1150–1159.

Guedez, L., Rivera, A.M., Salloum, R., Miller, M.L., Diegmueller, J.J., Bungay, P.M., and Stetler-Stevenson, W.G. (2003). Quantitative Assessment of Angiogenic Responses by The Directed in Vivo Angiogenesis Assay. The American Journal of Pathology *162*, 1431–1439.

Katoh, S., McCarthy, J.B., and Kincade, P.W. (1994). Characterization of soluble CD44 in the circulation of mice. Levels are affected by immune activity and tumor growth. J Immunol *153*, 3440–3449.

Kodama, K., Horikoshi, M., Toda, K., Yamada, S., Hara, K., Irie, J., Sirota, M., Morgan, A.A., Chen, R., Ohtsu, H., et al. (2012). Expression-based genome-wide association study links the receptor CD44 in adipose tissue with type 2 diabetes. Proc. Natl. Acad. Sci. U.S.A. *109*, 7049–7054.

Kothapalli, D., Zhao, L., Hawthorne, E.A., Cheng, Y., Lee, E., Pure, E., and Assoian, R.K. (2007). Hyaluronan and CD44 antagonize mitogen-dependent cyclin D1 expression in mesenchymal cells. J. Cell Biol. *176*, 535–544.

Lallemand, D., Curto, M., Saotome, I., Giovannini, M., and McClatchey, A.I. (2003). NF2 deficiency promotes tumorigenesis and metastasis by destabilizing adherens junctions. Genes Dev. *17*, 1090–1100.

Lennon, F.E., Mirzapoiazova, T., Mambetsariev, N., Mambetsariev, B., Salgia, R., and Singleton, P.A. (2014).

Transactivation of the receptor-tyrosine kinase ephrin receptor A2 is required for the low molecular weight hyaluronan-mediated angiogenesis that is implicated in tumor progression. J Biol Chem *289*, 24043–24058.

Loges, S., Schmidt, T., and Carmeliet, P. (2010). Mechanisms of resistance to anti-angiogenic therapy and development of third-generation anti-angiogenic drug candidates. Genes Cancer *1*, 12–25.

Mancuso, M.R., Davis, R., Norberg, S.M., O'Brien, S., Sennino, B., Nakahara, T., Yao, V.J., Inai, T., Brooks, P., Freimark, B., et al. (2006). Rapid vascular regrowth in tumors after reversal of VEGF inhibition. J. Clin. Invest. *116*, 2610–2621.

Mayer, S., Hausen, A. zur, Watermann, D.O., Stamm, S., Jäger, M., Gitsch, G., and Stickeler, E. (2008). Increased soluble CD44 concentrations are associated with larger tumor size and lymph node metastasis in breast cancer patients. J Cancer Res Clin Oncol *134*, 1229–1235.

Morrison, H., Sherman, L.S., Legg, J., Banine, F., Isacke, C., Haipek, C.A., Gutmann, D.H., Ponta, H., and Herrlich, P. (2001). The NF2 tumor suppressor gene product, merlin, mediates contact inhibition of growth through interactions with CD44. Genes Dev *15*, 968–980.

Murakami, D., Okamoto, I., Nagano, O., Kawano, Y., Tomita, T., Iwatsubo, T., De Strooper, B., Yumoto, E., and Saya, H. (2003). Presenilin-dependent γ-secretase activity mediates the intramembranous cleavage of CD44. Oncogene *22*, 1511–1516.

Okamoto, I., Kawano, Y., Tsuiki, H., Sasaki, J., Nakao, M., Matsumoto, M., Suga, M., Ando, M., Nakajima, M., and Saya, H. (1999). CD44 cleavage induced by a membrane-associated metalloprotease plays a critical role in tumor cell migration. Oncogene *18*, 1435–1446.

Päll, T., Gad, A., Kasak, L., Drews, M., Strömblad, S., and Kogerman, P. (2004). Recombinant CD44-HABD is A Novel And Potent Direct Angiogenesis Inhibitor Enforcing Endothelial Cell-Specific Growth Inhibition Independently of Hyaluronic Acid Binding. Oncogene *23*, 7874–7881.

Peterson, R.S., Andhare, R.A., Rousche, K.T., Knudson, W., Wang, W., Grossfield, J.B., Thomas, R.O., Hollingsworth, R.E., and Knudson, C.B. (2004). CD44 modulates Smad1 activation in the BMP-7 signaling pathway. J. Cell Biol. *166*, 1081–1091.

Pink, A., Kallastu, A., Turkina, M., Skolnaja, M., Kogerman, P., Päll, T., and Valkna, A. (2014). Purification, Characterization And Plasma Half-Life of Pegylated Soluble Recombinant Non-HA-Binding CD44. Biodrugs *28*, 393–402.

Porsch, H., Mehić, M., Olofsson, B., Heldin, P., and Heldin, C.H. (2014). Platelet-derived growth factor β-receptor, transforming growth factor β type I receptor, and CD44 protein modulate each other's signaling and stability. J. Biol. Chem. *289*, 19747–19757.

Protin, U., Schweighoffer, T., Jochum, W., and Hilberg, F. (1999). CD44-deficient mice develop normally with changes in subpopulations and recirculation of lymphocyte subsets. J Immunol *163*, 4917–4923.

Ristamäki, R., Joensuu, H., Salmi, M., and Jalkanen, S. (1994). Serum CD44 in malignant lymphoma: an

association with treatment response. Blood *84*, 238–243.

Rohan, R.M., Fernandez, A., Udagawa, T., Yuan, J., and D'Amato, R.J. (2000). Genetic heterogeneity of angiogenesis in mice. The FASEB Journal *14*, 871–876.

Rouschop, K.M.A., Roelofs, J.J.T.H., Claessen, N., da Costa Martins, P., Zwaginga, J.-J., Pals, S.T., Weening, J.J., and Florquin, S. (2005). Protection against renal ischemia reperfusion injury by CD44 disruption. J Am Soc Nephrol *16*, 2034–2043.

Scharpfenecker, M., Dinther, M. van, Liu, Z., Bezooijen, R.L. van, Zhao, Q., Pukac, L., Lowik, C.W., and Dijke, P. ten (2007). BMP-9 signals via ALK1 and inhibits bFGF-induced endothelial cell proliferation and VEGF-stimulated angiogenesis. J. Cell. Sci. *120*, 964–972.

Tanikawa, R., Tanikawa, T., Hirashima, M., Yamauchi, A., and Tanaka, Y. (2010). Galectin-9 induces osteoblast differentiation through the CD44/Smad signaling pathway. Biochem. Biophys. Res. Commun. *394*, 317–322.

Teriete, P., Banerji, S., Noble, M., Blundell, C.D., Wright, A.J., Pickford, A.R., Lowe, E., Mahoney, D.J., Tammi, M.I., Kahmann, J.D., et al. (2004). Structure of the regulatory hyaluronan binding domain in the inflammatory leukocyte homing receptor CD44. Mol Cell *13*, 483–496.

Tremmel, M., Matzke, A., Albrecht, I., Laib, A.M., Olaku, V., Ballmer-Hofer, K., Christofori, G., Heroult, M., Augustin, H.G., Ponta, H., et al. (2009). A CD44v6 peptide reveals a role of CD44 in VEGFR-2 signaling and angiogenesis. Blood *114*, 5236–5244.